

Effect of Prestrain on Formability and Forming Limit Strains During Tube Hydroforming

C. Nikhare¹ and K. Narasimhan²

Abstract: The tube hydroforming process is a relatively complex manufacturing process; the performance of this process depends on various factors and requires proper combination of part design, material selection and boundary conditions. In manufacturing of automotive parts, such as engine cradles, frames rails, sub-frames, cross members, and other parts from circular tubes, pre-bending and pre-forming operations are often required prior to the subsequent tubular hydroforming process to fit the tubular blank in the complex die shape. Due to these pre-hydroforming operations, some of the strains are already developed before going to the actual hydroforming process. Such developed strains before hydroforming process in the part is called as prestrain. In this paper the study of effect of prestrain on formability and forming limit strains during tube hydroforming is done by simulation by taking the material prestrain value. The forming limit strains of pre-strained tube during hydroforming are predicted. A series of tube bulge tests for tube hydroforming are simulated by a commercial finite element solver to predict the limit strains. Numerical simulation of forming limit strains in tube hydroforming with different internal pressure and different simulation set up with or without axial feeding are considered to develop wide range of strain paths in the present work. The effects of process conditions on the forming limit strains are detailed. In this paper the forming limit strains during tube hydroforming are simulated for prestrain and compared with zero prestrain. Prediction of limit strains is based on a novel thickness based necking criterion.

Keyword: Hydroforming, limit strains, pre-strain.

1 Introduction

During metal forming operations, the material is subjected to complex strain histories. The study of the response of a material undergoing a sequence of loadings is thus important for the knowledge of its macroscopic behavior. The response of a pre-strained material is the result of an interaction between its structural state and the new loading mode [Raphanel, Rauch, Shen and Schmitt (1987)]. Automotive stampings are often subjected to multiple forming operations. Single mode deformation processes, most commonly used in laboratory evaluations of automotive sheet materials, may not realistically predict material press performance. Therefore, formability tests that use multiple deformation stages would better simulate actual material performance. Also, by suitably modifying the process steps and strain paths it might be possible to achieve the desired product shape even when the formability of the material, as measured by simpler formability tests, is limited. The usual technique has been to deform or pre-strain a specimen to some level of total plastic strain in one linear proportional strain path, to halt the straining of specimen, and then to reload the specimen in another linear proportional strain path [Jain, Allin, Duan and Lloyd (2005)].

The plastic flow behavior of metals during sequential strain paths has been exhaustively analyzed. The aspects of mechanical behavior associated with the strain path changes are now well known. The mechanical behavior of metals after path changes follows the following pattern: the higher the initial flow stress in reloading the lower the workhardening rate and the total uniform plas-

¹ Department of Metallurgical Engineering & Materials Science, IIT BOMBAY, Powai, Mumbai 400 076, INDIA

² Corresponding author. Email: nara@iitb.ac.in

tic deformation, during the complex path. The empirical equation that accurately describes the experimental stress–strain curves of pre-strained sample is a Swift type equation that, taking into account the monotonic behavior in tension and the values of the normalized reloading yield stress, predicts the work-hardening behavior after pre-strain. The non-uniform deformation sometimes observed at the beginning of the reloading in tension, before the maximum load is attained, is not connected with local instability at the grain level. The experimental analyses indicates that this effect consists of a delay in starting deformation in some regions, whose deformations evolve differently along the sample and must be related with the mechanical behavior and the presence of geometrical defects. In order to get a better understanding of this effect, further analyses are needed. However, the experimental measurement of the evolution of the strain distribution along the samples, during tensile tests, needs specific analysis that is not simple to perform with common test equipment. In this context, the numerical simulation is a powerful alternative tool if correct mechanical models are used [Menzes, Fernandes and Rodrigues (1999)].

The hydroforming process has become an effective manufacturing process, because it can be adapted to the manufacturing of complex structural components into a single body with high structural stiffness. Tube hydroforming has been successfully developed in industry such as in the manufacturing of the components of automotive vehicles. Steel tube has excellent strength to weight ratio and therefore its applications can effectively reduce vehicle weight and improve vehicle stiffness. Other potential advantages are improved dimensional control and reduced cost, both of which are partially due to part consolidation and a large reduction in the welding of stampings to create closed sections [Chen, Soldaat and Moses (2004)].

The full exploitation of hydroforming requires improved understanding of forming limits during hydroforming process. In this paper, the effect of pre-strained tube on formability and forming limit strains during tube hydroforming is predicted and

compared with zero pre-strained tube.

2 Material and Methodology

2.1 Material

The studied deep drawing quality steel material considered for the present work. The pertinent material properties are shown in Tab. 1.

Table 1: Material properties assumed for simulations

n	K (MPa)	Y_s (MPa)	R_0	R_{45}	R_{90}	Young's Modulus (GPa)	Poisson's Ratio	Thickness (mm)
0.238	645	211	1.09	0.79	1.29	206	0.33	1.4

2.2 Methodology

The methodology adopted in the simulation of tube hydroforming is tube bulge test. The simulations have been carried out on the zero pre-strain and pre-strain tube. Different effective prestrain value used are 0.2, 0.3 and 0.4 and to get the wide range of forming limit curve, different strain paths used are biaxial tension, plain strain and uniaxial tension.

2.2.1 Tube Bulge Test

In order to evaluate the forming limit strains during tube hydroforming, the tube bulge test is simulated. These tests use the internal hydraulic pressure to bulge the tube that is supported between a lower and an upper die. The lower part of the die is fixed in movement, while the other is free to move. The two punches in the axial direction of the tube provide for axial feeding [Song, Kim, Kim and Kang (2005); Kim, Kim, Song and Kang (2005); Kim, Kang, Hwang and Park (2004) and Kim, Kim, Song and Kang (2004)]. The following three boundary conditions help to achieve different strain paths: 1) fixed expansion 2) free expansion and 3) axial feed expansion of tubes with different aspect ratios. High internal pressures under relatively low axial feeding will be required to observe the bursting failure. All list conditions will be simulated using FE based code. A novel

thickness gradient based criterion is used for predicting the limit strains in the simulation.

2.2.1.1 Fixed expansion of tubes

In fixed tube expansion, the tube is fixed between the two dies (i.e. Die1 and Die2) by giving the coefficient of friction between the tube and dies as 0.5, Fig. 1. When the hydraulic pressure builds up in the tube, it expands in the middle portion without any material feed-in. This operation is completely a stretching operation. This test is performed for different aspect ratios (i.e. expansion zone/tube diameter [l/d ratio = 1 to 1.8]).

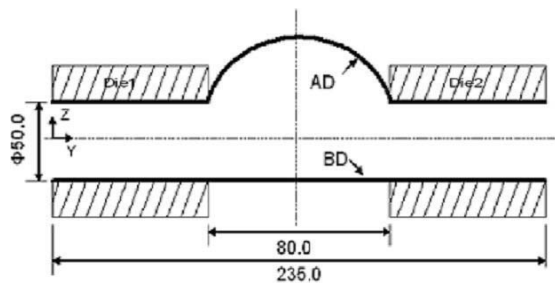


Figure 1: Fixed tube expansion in Hydroforming BD – Before deformation AD – After Deformation

2.2.1.2 Free expansion of tubes

In this case, the tube is free to move in the dies (i.e. Die1 and Die2). The coefficient of friction between the tube and the die is assumed as 0.12. This test is performed without and with the middle die portion as shown in Fig. 2 and Fig. 3. When the hydraulic pressure builds up in the tube, the tube expands in the middle portion with material fed in due to force exerted by internal pressure. This test is also performed for different aspect ratios (i.e. l/d ratio = 1 to 1.8).

2.2.1.3 Axial feed expansion of tubes

In axial feed expansion of tubes, the tube is simulated for simultaneous application of internal pressures and axial forces from both ends of tubes. The coefficient of friction between the tube and dies is assumed as 0.12. This test is performed without and with the middle dies

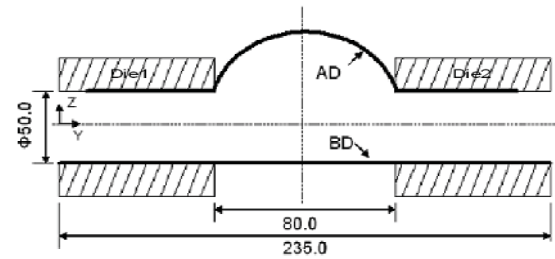


Figure 2: Free tube expansion in hydroforming without middle portion of die

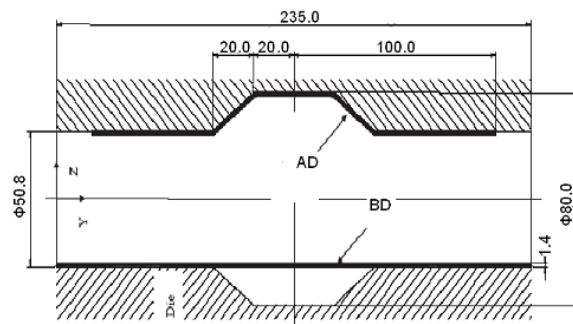


Figure 3: Free tube expansion in hydroforming with middle portion of die

portion as shown in Fig. 2 and Fig. 3. In this case, additional material feed is provided by two punches at the end of the tubes [Kulkarni, Biswas, Narasimhan, Luo, Mishra, Stoughton and Sachdev (2004)]. When the hydraulic pressure builds up in the tube, the tube expands in the middle portion with material fed in due to axial forces of punch1 and punch2. This test is also performed for different aspect ratio (i.e. l/d ratio = 1 to 1.8).

2.2.2 Effective strain

To simulate the prestrain tube with different effective prestrain value, like value of point 1, 2 and 3 of the yield locus as shown in Fig. 4 and the strain path of the tube before hydroforming used might be biaxial tension, plain strain and uniaxial tension as shown in Fig. 5. To simulate the prestrain tube during tube hydroforming, the assumption consider is that the tube outer bending is in uniaxial tension, like the strain path which is in condition 3, shown in Fig. 5. To consider the different tensile effective strain, von-Mises criterion is used to evaluate the thinning and the thickness

of the tubular blank. Tab. 2 shows the estimated % thinning and the thickness of the tube before hydroforming for different tensile effective strain.

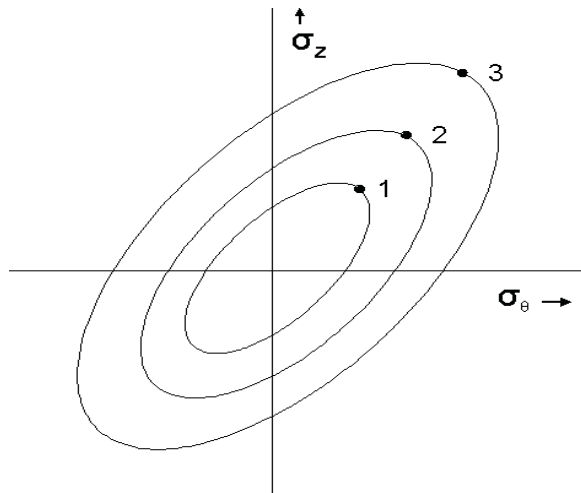


Figure 4: Yield locus with different prestrain conditions

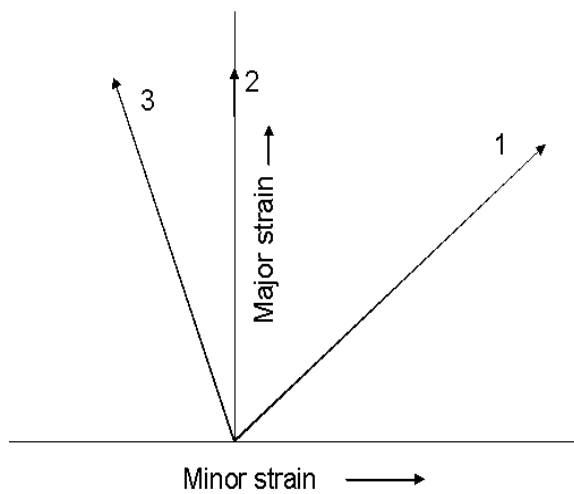


Figure 5: Different strain paths for simulation; 1 – biaxial tension, 2 – plane strain, 3 – uniaxial tension

2.2.3 Numerical simulation

The tube is assumed to be a circular cylinder for purpose of simulation. Variations of wall thickness and material property parameters around the circumference of the tube are neglected. The

Table 2: Thickness of tubular blank for different tensile effective strain

Tensile effective strain	% Thinning	Thickness (mm)
0	0	1.40
0.2	10	1.26
0.3	15	1.19
0.4	20	1.12

wall thickness of the tube is taken to be the average measured value of 1.4 mm. Similar relevant assumptions are used in pre-strained tube hydroforming processes. The wall thickness of the pre-strained tube is taken to be average measured value as 1.26, 1.19 and 1.12 corresponding to the thinning value as 0.1, 0.15 and 0.2 at effective pre-strain value coming as 0.2, 0.3 and 0.4 from von-Mises criterion. Fig. 6 shows the stress strain curve for zero pre-strain and pre-strain tube is according to flow equation, $\sigma = K(\epsilon_0 + \epsilon)^n$.

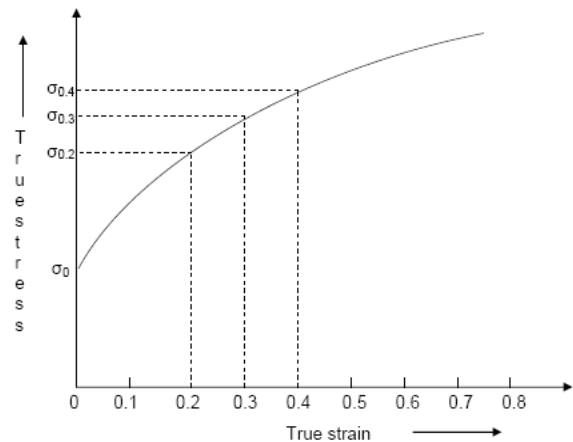


Figure 6: Numerical true stress – true strain curves with 0%, 20%, 30% and 40% pre-strain

Forming is simulated by using the FE based code PAM-STAMP2G 2004. Tube ends are free to move in the y-direction. The tube is allowed for radial expansion. Internal pressure and axial forces are applied simultaneously and proportionally. The calculated results, for all end conditions considered, are symmetrical to the mid-section of the tube. These symmetry results give added confidence in the accuracy of the numerical calculations obtained from the full model.

2.2.4 Thickness gradient criterion

To predict the forming limit strains coming from the simulation this work will follow the Thickness gradient criterion. During sheet metal forming a localized neck is perceived by the presence of a critical local thickness gradient in the sheet. Such a perception of the neck is independent of the strain path, rate of forming and the type of sheet metal (i.e. the material properties) being formed. The critical local thickness gradient R_{cri} , exists at the on – set of a visible local neck. After start of deformation, a thickness gradient, “ $R_{thickness\ gradient}$ ” develops in the deforming sheet which is expressed Eq. 1.

$$R_{thickness\ gradient} = \frac{\text{current thickness of necking element}}{\text{current thickness of neighboring element}} \quad (1)$$

As the deformation progresses, this thickness gradient keeps on reducing from initial value of 1.0. The thickness gradient becomes steeper at the on – set of localized necking and at this transition from diffused necking it attains a critical value. The criterion is represented in Eq. 2.

$$R_{thickness\ gradient} \leq R_{cri} \quad (2)$$

The R_{cri} is experimentally estimated as 0.92. If $R_{thickness\ gradient}$ is less than 0.92, the component is considered as necked [Kumar, Date and Narasimhan (1994) and Nandedkar (2000)].

3 Results and Discussion

Fig. 7 compares the input-output pressure curve obtained from FEA simulation. The sudden drop of output pressure is an indication of excessive thinning in the expansion region. The axial displacement vs. time applied during axial feed expansion of tubes is shown in Fig. 8.

In fixed expansion of tubes, when we reduce the aspect ratio and fix the pressure curve for different simulation, both the strains is increasing but with the combination of increase of pressure curves and fixed aspect ratio, the strains are decreasing. The axial stress and circumferential stress are generated simultaneously because the tube is not

allowed to feed in the expansion zone. Thus strain develops in stretching domain.

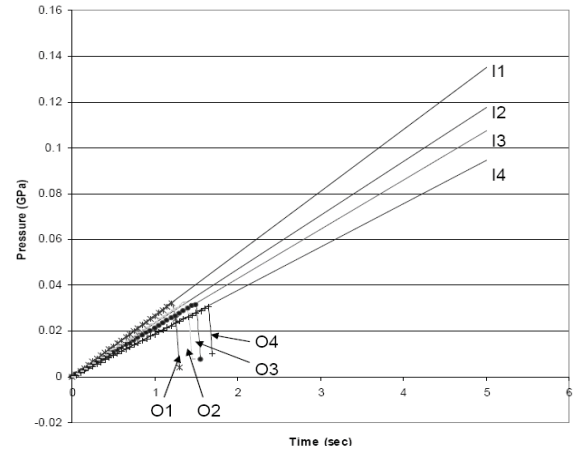


Figure 7: Input – Output pressure - time histories during hydroforming

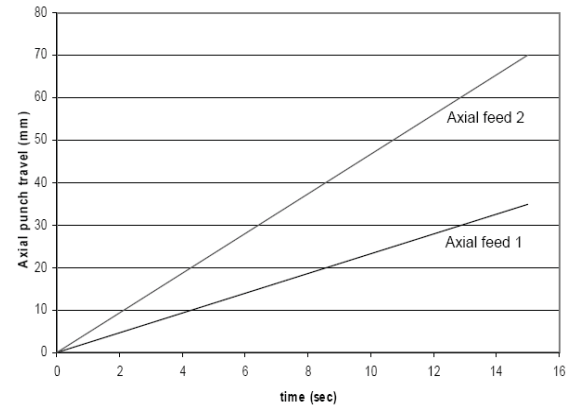


Figure 8: Axial punch displacement during axial feed hydroforming

In free expansion of tubes, as soon as we reduce the aspect ratio the strains are increasing but the value of strains are more. As the dominant stress here is circumferential stress and also the tube is free to feed in, the value of strains are more than in fixed expansion of tubes, but the percentage change of the major strain is less than the minor strain when compared with fixed expansion of tubes. When the aspect ratio is fixed and the pressure curves increased, the tube is self fed in as per the force generated by the fluid pressure on

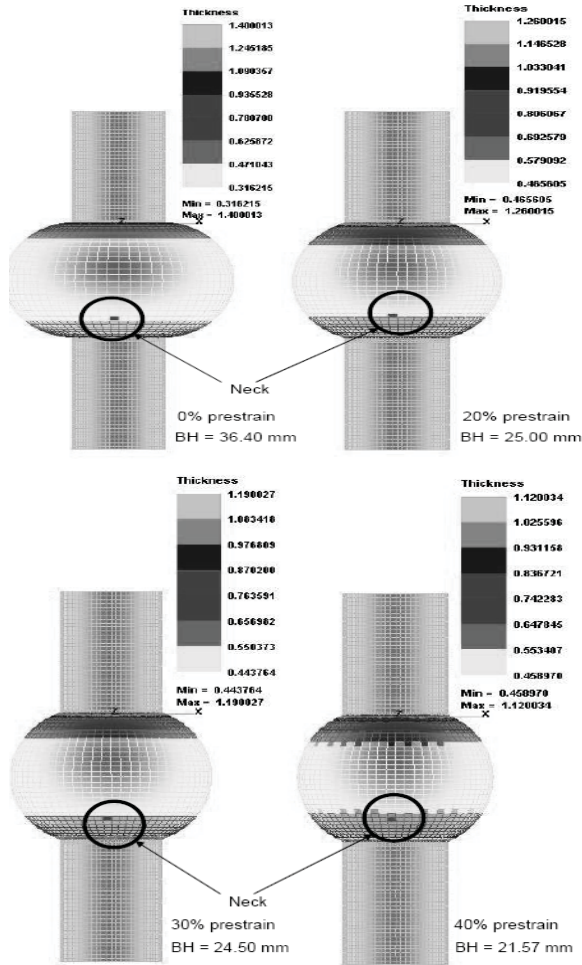


Figure 9: Simulation necked tubes obtained from bulge test under different pre-strain conditions; BH–Bulge Height

the tube material. So in this case the circumferential stress dominates the axial stress, so that is why the percentage change of major strain is less than minor strain when compared with fixed expansion of tubes. Here the strain path leads towards plane strain conditions.

In axial feed expansion of tubes, for different aspect ratio, the strains decrease in same manner as in fixed expansion of tubes and free expansion. So, for various combinations of axial feed and internal pressure curves we obtain limit strains in stretching, in plane strain and mostly in drawing zone when the die support is used.

Fig. 9 shows the results of excessive pressuriza-

ing during the bulging process, necking occurs at the middle of the tube wall as per the thickness gradient criterion. The picking of neck point at a particular time by thickness gradient criterion is the same at which the output internal pressure of tubes drops as per the Fig. 7, verifying the on-set of neck.

Tab. 3 shows the details of bulge height at necking at different pre-strained conditions under different loading paths during tube hydroforming. The table clearly shows that as the % pre-strain increases, the bulge height decreases. Hence, the formability decreases as the % pre-strain increases. Tab. 4 shows the details of necking or bursting pressure at different pre-strained tube under different loading paths during tube hydroforming. It indicates that the necking pressure is almost same for pre-strained tube i.e. the time require to satisfying the thickness gradient criterion is almost same for each loading path.

Table 3: Details of Bulge Height at necking at different pre-strained tube under different loading paths during tube hydroforming simulations

case % prestrain	Bulge Height (mm)			
	I1	I2	I3	I4
0%	36.40	31.67	35.45	37.78
20%	25.00	28.11	26.34	27.14
30%	24.50	26.81	23.87	23.31
40%	21.57	23.75	21.16	20.76

Table 4: Details of necking pressure at different pre-strained tube under different loading paths during tube hydroforming simulations

case % prestrain	Necking Pressure (MPa)			
	I1	I2	I3	I4
0%	32.90	32.40	31.27	30.80
20%	36.00	34.80	32.80	33.60
30%	36.00	36.00	35.20	34.50
40%	36.00	34.82	35.20	34.53

Fig. 10 shows how the thickness gradient is developed with respect to time from case I1 to I4. It also shows that the necking pressure is continuously decreasing from I1 to I4, is the matter of fact of optimization for a particular combination of process conditions and the material properties.

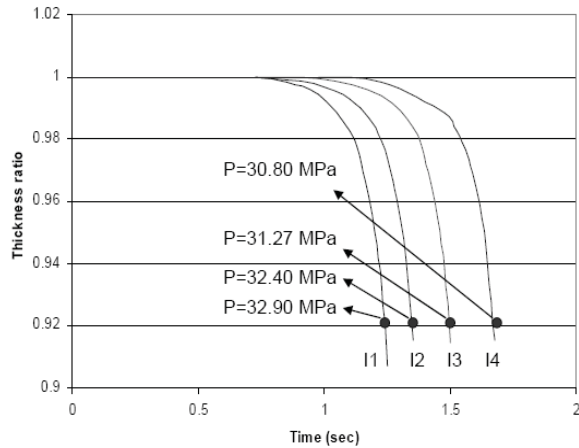


Figure 10: Thickness ratio along time during tube hydroforming under different loading paths

The gradient of thickness during tube hydroforming at different pre-strained tube under different loading path is shown in Fig. 11. It straight away clears that for 0% pre-strain the thickness gradient develops faster than the pre-strain tube, but the thickness gradient during pre-strain tube hydroforming are almost same and the thickness gradient criterion satisfies at the almost same time. The necking bulge height which is shown in Tab. 3 is decreasing for the same pressure curve is because if the % pre-strain is more, the work hardening is more. So, the failure of the tube is delayed as we go towards 0% pre-strain.

Tab. 5 presents the strain conditions defined for the various tube hydroforming simulations at 0% pre-strain. Thus in this way a wide range of limit strains from drawing to complete stretching is obtained. Fig. 12 shows the comparison of limit strains during tube hydroforming for 0% pre-strain with thickness 1.4 mm, 1.12 mm and 40% pre-strain with thickness 1.12 mm. The graph clearly shows that the limit strains during tube hydroforming at 0% pre-strain are higher than that at 40% pre-strain, but the difference is

the combination of pre-strain plus thickness effect. Fig. 13 shows the comparison of limit strains at different level of pre-strain. It clearly shows that as the % pre-strain increases, the limit strains decreases.

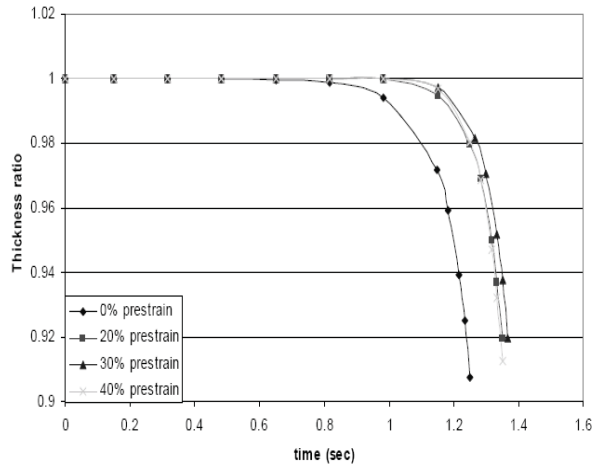
Table 5: Details of different simulations during tube hydroforming; FA – Axial feed expansion, FR – Free expansion, FI – Fixed expansion

Sr. No	Boundary Conditions	Emaj	Emin	Emin/Emaj
1	FA	0.8356	-0.2206	-0.2640
2	FA	0.7030	-0.1672	-0.2378
3	FA	0.6820	-0.1588	-0.2328
4	FA	0.5472	-0.1083	-0.1979
5	FA	0.4385	-0.0170	-0.0387
6	FA	0.3739	0.0410	0.1096
7	FA	0.3583	0.0609	0.1699
8	FA	0.3363	0.0803	0.2387
9	FR	0.3390	0.1080	0.3185
10	FR	0.3901	0.1870	0.4793
11	FI	0.4877	0.2644	0.5421
12	FI	0.5282	0.3018	0.5713
13	FI	0.6760	0.4139	0.6122
14	FI	0.7117	0.4330	0.6084
15	FI	0.8257	0.5188	0.6283
16	FI	0.8980	0.5748	0.6400

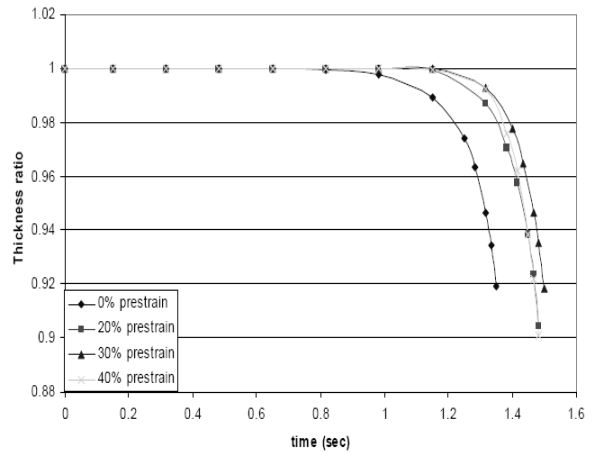
The four graphs in Fig. 14 are the thickness strain distribution for the particular loading path for the same bulge height. It shows that, as the pre-strain increases, the thickness strain decreases, gives the confirmation that the limit strain are decreasing as we go towards higher pre-strain.

4 Conclusions

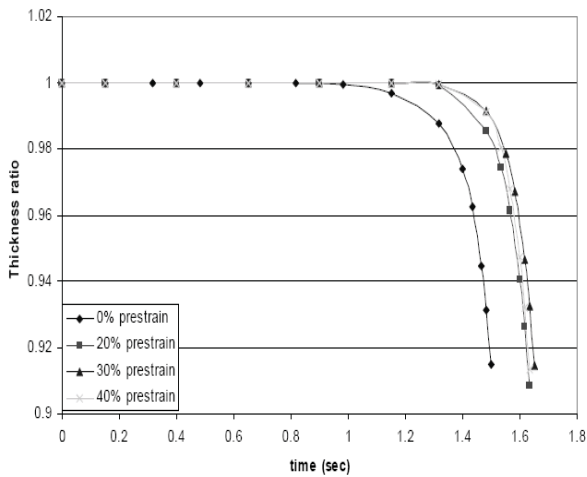
In order to evaluate the forming limit strains during hydroforming process, simulation under various combinations of internal pressure and axial loading and different process conditions were studied. Using thickness gradient criterion, the occurrence of necking i.e. forming limit strains



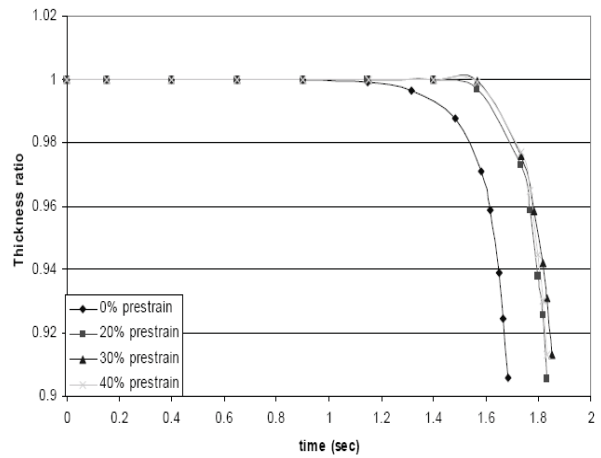
(a) For pressure curve I1



(b) For pressure curve I2



(c) For pressure curve I3



(d) For pressure curve I4

Figure 11: Thickness ratio along time during tube hydroforming at different pre-strained tube under different loading paths (I1, I2, I3 and I4); FA – Axial feed expansion, FR - Free expansion, FI – Fixed expansion

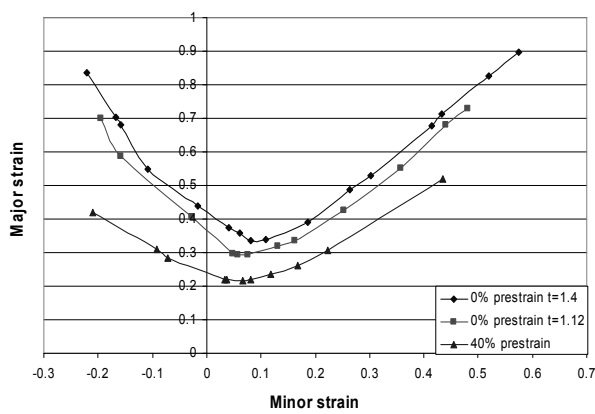


Figure 12: Forming limit curve for 0% and 40% pre-strain of same thickness

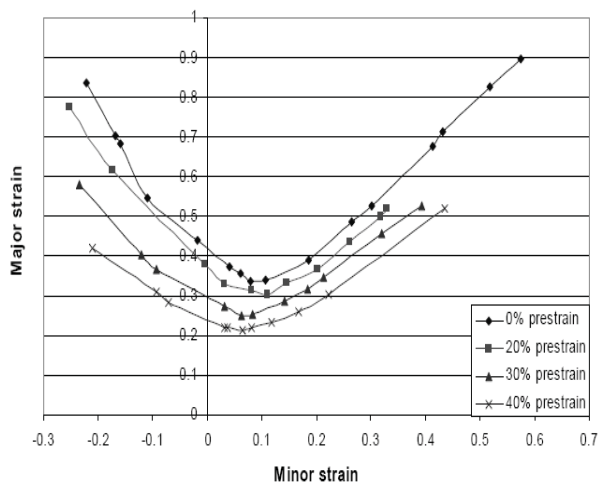


Figure 13: Forming limit curve for different pre-strained tube during tube hydroforming

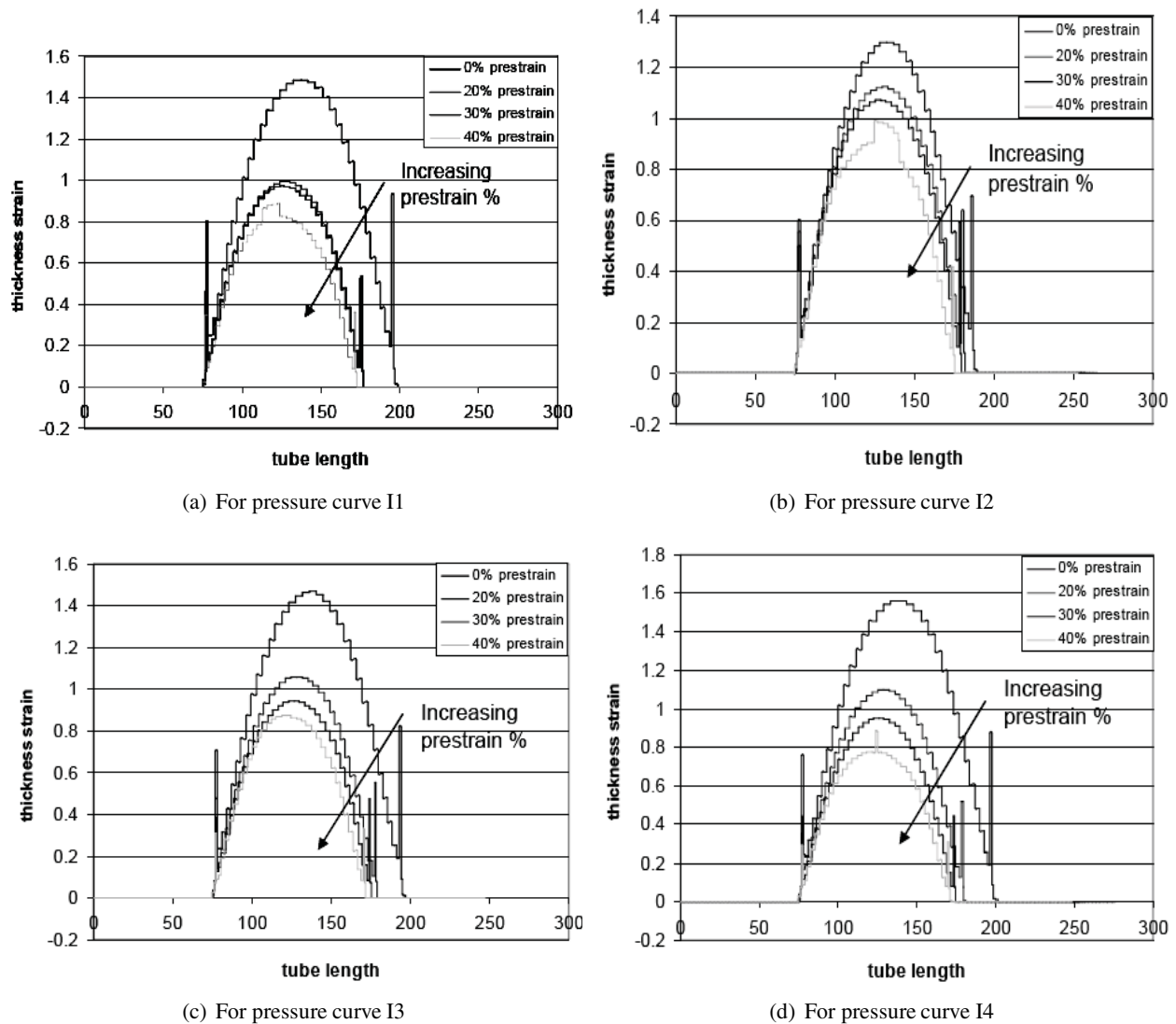


Figure 14: Thickness strain distribution along tube length during tube hydroforming under different prestrained tube under different loading paths (I1, I2, I3 and I4)

during tube hydroforming at different pre-strain levels under different loading paths were estimated. Comparison of formability and forming limit strains during tube hydroforming at different % of pre-strain value shows that the formability and forming limit strains decrease with increase in magnitude of prestrain.

Acknowledgement: Authors thank funding support from CAR-TIFAC project grant number 05TI002.

References

- Chen, K. K.; Soldaat, R. J.; Moses, R. M.** (2004): Free expansion bulge testing of tubes for automotive hydroform applications. *SAE Technical Paper Series*, 2004-01-0832.
- Jain, M.; Allin, J.; Duan, X.; Lloyd, D. J.** (2005): Effect of reverse dome stretching on dome height and forming limits of sheet materials. *Materials Science and Engineering A*, vol 390, pp. 210–216.
- Kim, J.; Kim, S. W.; Song, W. J.; Kang, B. S.** (2005): Analytical and numerical approach to

prediction of forming limit in tube hydroforming. *International Journal of Mechanical Sciences*, vol 47, pp. 1023 – 1037.

Kim, J.; Kang, B. S.; Hwang, S. M.; Park, H. J. (2004): Numerical prediction of bursting failure in tube hydroforming by the FEM considering plastic anisotropy. *Journal of Materials Processing Technology*, vol 153–154, pp. 544–549.

Kim, J.; Kim, S. W.; Song, W. J.; Kang, B. S. (2004): Analytical approach to bursting in tube hydroforming using diffuse plastic instability. *International Journal of Mechanical Sciences*, vol 46, pp. 1535–1547.

Kulkarni, A.; Biswas, P.; Narasimhan, R.; Luo, A. A.; Mishra, R. K.; Stoughton, T. B.; Sachdev, A. K. (2004): An experimental and numerical study of necking initiation in aluminum alloy tubes during hydroforming. *International Journal of Mechanical Sciences*, vol 46, pp. 1727–1746.

Kumar, S.; Date, P. P.; Narasimhan, K. (1994): A new criterion to predict necking failure under biaxial stretching. *Journal of Materials Processing Technology*, vol 45, pp. 583.

Menzes, L. F.; Fernandes, J. V.; Rodrigues, D. M. (1999): Numerical simulation of tensile tests of prestrained sheets. *Materials Science and Engineering A*, vol 264, pp. 130–138.

Nandedkar, V. (2000): Formability Studies on a Deep Drawing Quality Steel. *Ph. D. Thesis IIT-Bombay*.

Raphanel, J. L.; Rauch, E.; Shen, E. L.; Schmitt, J. –H. (1987): Shear of prestrained steel specimens. *Scripta Metallurgica*, vol 21, pp. 1087–1090.

Song, W. J.; Kim, S. W.; Kim, J.; Kang, B. S. (2005) Analytical and numerical analysis of bursting failure prediction in tube hydroforming. *Journal of Materials Processing Technology*, vol 164–165, pp. 1618–1623.